16th World Conference on Earthquake Engineering, 16WCEE 2017

Santiago Chile, January 9th to 13th 2017

Paper N° 3098

Registration Code: S-J1465948316

STIFFNESS DECAY AND DAMPING RATIOS OF STEEL FIBER REINFORCED CONCRETE WALLS

J. Carrillo[(1)], J. Pincheira[(2)] , S. Alcocer[(3)]

[(1)] *Associate Professor, Department of Civil Engineering, Universidad Militar Nueva Granada, Colombia, wjcarrillo@gmail.com*
[(2)] *Associate Professor, Dep. of Civil and Environmental Engineering, Univ. of Wisconsin-Madison, USA, jose.pincheira@wisc.edu*
[(3)] *Research Professor, Institute of Engineering, Universidad Nacional Autónoma de México, UNAM, salcocerm@ii.unam.mx*

Abstract

The stiffness degradation and damping ratio characteristics of low-rise steel fiber-reinforced concrete (SFRC) walls subjected to shake table excitations is presented in this paper. Three fiber volume contents (0.55, 0.75, and 1 %) and fibers with aspect ratios (length-to-diameter ratio) of 64 and 80 were used to fabricate six SFRC walls. The results of two conventionally reinforced concrete (RC) walls are included as a benchmark. Wall performance is presented in terms of observed failure modes, measured lateral drift components, fundamental frequencies, damping factors, and stiffness decay relationships. The data show that larger drift ratios can be achieved as the fiber content increased, irrespective of the fiber type, and that fibers with a higher aspect ratio led to a greater number, smaller crack widths. Stiffness reductions in the order of 50% were observed for the SFRC walls at relatively small lateral drifts (0.1 to 0.2%). Nonetheless, SFRC walls showed smaller stiffness reductions than the companion RC walls over the entire range of drifts. Measured damping ratios for the SFRC walls showed wide scatter, but ranged between 6% at low drifts and as high as 12% after diagonal cracking at larger drifts. The conventionally reinforced concrete walls showed similar values at low drifts, but somewhat less values (10%) at larger drifts.

Keywords: steel fibers; reinforced concrete walls; stiffness degradation; damping, period of vibration.

1. Introduction

The use of Steel Fiber-Reinforced Concrete for enhancing the response of earthquake resistant members has gradually gained acceptance in recent years. SFRC has been shown to have the potential to increase member shear strength and deformation capacity, and to reduce the amount of structural damage induced by earthquake-induced actions. In a recent investigation, the seismic performance of SFRC walls was studied experimentally [1, 2]. A total of six SFRC walls were built and tested under shaking table excitations. Each wall was fabricated with a different type of steel fiber or fiber volume. In addition, two reinforced concrete walls were tested under the same excitations as a benchmark for comparing the behavior of conventionally reinforced walls with that of the SFRC walls.

Many studies have shown that reinforced concrete, RC, members subjected to repeated cycles of inelastic displacement are affected by stiffness and strength degradation, as well as pinching of the hysteresis loops [3, 4, 5]. The amount of degradation depends on the displacement amplitude and the number of cycles experienced by the member under a given displacement amplitude, as well as on the member reinforcing details. Less known are the degradation characteristics of steel fiber-reinforced concrete members. The main focus of this paper is to assess the observed stiffness degradation characteristics and damping ratios of SFRC walls with various fiber volume contents subjected shake-table tests. Wall performance is discussed in terms of failure modes, lateral drift components, measured fundamental frequencies and stiffness decay relationships, and damping ratios.

2. Experimental program

Six wall specimens with different fiber reinforcement characteristics (fiber type and content) were tested under three ground motions. In addition, a wall reinforced with deformed bars (DB) and a wall reinforced with welded wire reinforcement (WWR) in the web were also tested. Specimen geometry was based on the walls commonly found in a two-story housing unit. In this type of housing, wall thickness and clear height are commonly 100 and 2400 mm, respectively. The floors often consist of 100-mm thick solid, cast in-place, slabs, though hollow core slabs are also sometimes used. Foundations are strip footings made of 400-mm square RC beams that support a 100-mm thick floor slab.

Because of the limitations in the payload capacity of the shaking table, the size of wall models was reduced to 80% of the walls in an actual housing unit. The simple law of similitude was used for scaling specimens. For this type of simulation, models are built with the same materials of the actual walls and only the dimensions are modified. Specimen geometry, reinforcement, material properties, and the test protocol are presented as follows. Further details of the experimental program may be found in Carrillo *et al*. [1], and Carrillo and Alcocer [6].

2.1 Geometry and reinforcement of walls

Nominal geometry and reinforcement layout of the specimens are shown in Fig. 1. According to the scaling factors to satisfy the law of similitude, wall height, length, and thickness were calculated as 1920 mm, 1920 mm, and 80 mm, respectively. Wall specimens were cast on top of a stiff, reinforced concrete foundation beam which was later used to anchor the specimens to the shake table platform. A top slab, cast monolithically with the walls, was used to connect the mass-carrying load system during the tests.

Main dimensions and characteristics of the SFRC used in the specimens are summarized in Table 1. Hook-ended steel fibers with a length-to-diameter ratio, l_f/d_f, of either 64 (type 1F, l_f = 35 mm, d_f = 0.55 mm) or 80 (type 2F, l_f = 60 mm, d_f = 0.75 mm) were used. Three fiber contents, namely 0.55, 0.75, and 1.0% were studied with each fiber type for a total of six SFRC wall specimens.

The geometry and reinforcement in the boundary elements (longitudinal and transverse) of walls with deformed bars or welded wire reinforcement in the web (specimens MCN100 and MCN50m in Table 1) were roughly the same as those of the SFRC specimens. In the web, however, wall MCN100 was reinforced with a single layer of No. 3 deformed bars (9.5 mm diameter) spaced at 320 mm in both, the horizontal and vertical directions (Fig. 1b), which approximately corresponds to a web reinforcement ratio of 0.26% (i.e., the minimum ratio required by ACI 318-14 [7].

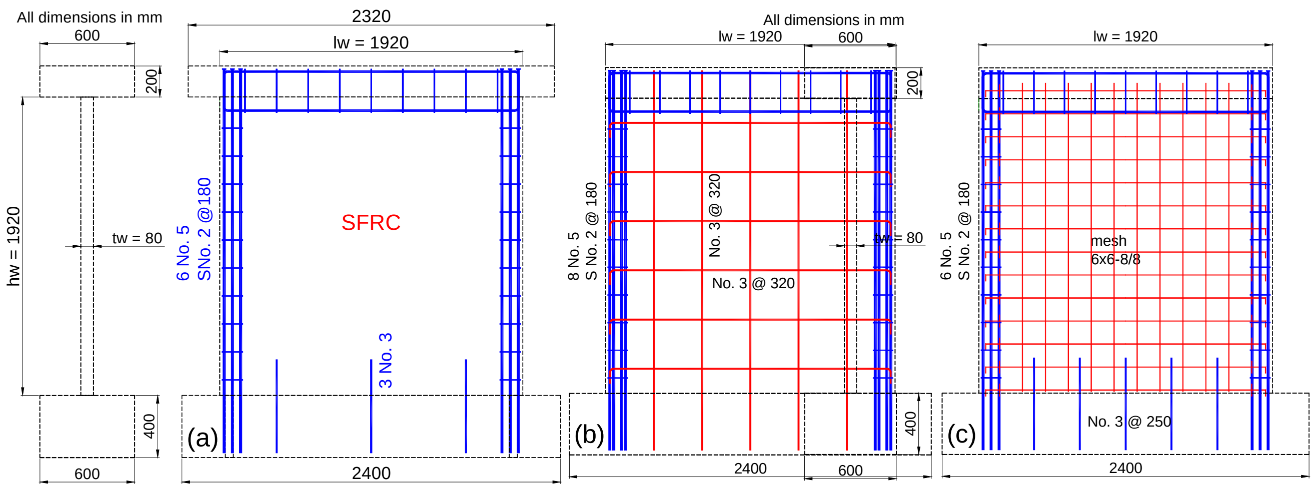

Fig. 1 – Geometry and reinforcement layout: (a) SFRC walls, (b) wall with deformed bars in the web, (c) wall with welded wire reinforcement in the web.

Wall MCN50m was reinforced with a single layer of No. 8 welded wires (4.1 mm diameter) spaced at 150 mm (6 in.), which approximately corresponds to 50% of the minimum web reinforcing ratio required by ACI 318-14 [7]. This was done to study the behavior of these substandard reinforced walls in response to the observed construction practice of these residential units in some regions of Latin America. Web reinforcement in these two walls was placed centered within the wall thickness. In addition, same ratios of horizontal and vertical web reinforcement were used in these benchmark walls.

Table 1 – Main characteristic of the wall specimens

Specimen designation		Web reinforcement type	Fiber content *		ρ_w (%)	Wall dimensions			
			(kg/m³)	(%)		t_w (mm)	h_w (mm)	l_w (mm)	h_w/l_w (mm)
SFRC Walls	MC1F0.55	Steel fibers Type 1F	45	0.55	-	80	1920	1920	1.0
	MC1F0.75		60	0.75	-	81	1921	1924	1.0
	MC1F1.00		75	1.00	-	84	1918	1925	1.0
	MC2F0.55	Steel fibers Type 2F	45	0.55	-	82	1925	1919	1.0
	MC2F0.75		60	0.75	-	81	1921	1917	1.0
	MC2F1.00		75	1.00	-	81	1920	1916	1.0
RC Walls	MCN100	Deformed bars (#3@320mm)	-		0.26	84	1924	1921	1.0
	MCN50m	Welded wires (W2@150mm)	-		0.11	83	1923	1916	1.0

* Nominal values. See measured values in Table 2.

2.2 Mechanical properties of SFRC walls

The specified compressive strength of the SFRC was chosen as 25 MPa as is commonly used in the walls of these residential units. The SFRC was ready-mixed at the concrete plant when a 0.55% volume fraction of fibers was planned. In specimens cast with 0.75% and 1.0% fiber volume fractions, however, the fibers were added in-situ to the concrete mixture. Mean value of the measured mechanical properties of the plain concrete (i.e., prior to adding the fibers) and the SFRC mixtures are presented in Table 2. Properties were obtained from compression tests of standard cylinders, and from third-point loading flexural tests of prismatic beams in accordance with ASTM C-1609 [8]. All properties were measured on the same day that the shake table tests were conducted. As shown in Table 2, the measured residual strengths of the mixes was not always compliant with that required by

ACI 318-14 [7]. With type 1F fibers, only the mix with a fiber content of 1% was compliant, while with type 2F fibers, the mixes with 0.75% and 1% fiber content were compliant.

Table 2 – Measured mechanical properties of the concrete mixtures

Mechanical property	SFRC walls								RC walls
	1F				2F				
	V_f(%)				V_f(%)				V_f(%)
	0	0.55	0.75	1.00	0	0.55	0.75	1.00	0
Actual volume fraction of fibers, %	N.A.	0.52	0.76	1.00	N.A.	0.56	0.84	1.07	N.A.
Compressive strength, f'_c, MPa	*	22.2	21.0	20.3	35.6	31.1	30.8	30.7	24.8
Modulus of elasticity, E_c, MPa	*	9050	8508	8337	15857	10616	10615	12384	14760
First-peak flexural stress, f_r, MPa	4.04	3.19	3.69	3.35	3.99	3.49	4.03	4.37	3.75
Maximum flexural stress, f_{max}, MPa	4.04	3.23	3.69	3.96	3.99	3.49	4.42	5.41	3.75
$f_{lc/300} / f_r$	0	0.72	0.80	1.12	0	0.79	1.02	1.17	0
$f_{lc/150} / f_r$	0	0.65	0.65	0.85	0	0.66	0.94	1.02	0
Residual strength compliance	N.A.	No	No	Yes	N.A.	No	Yes	Yes	N.A.

2.3 Mechanical properties of RC walls

Mean values of the mechanical properties measured for the concrete mixture used in RC walls are included in Table 2. The specified yield strength of the deformed bars (No. 5 and No. 3) was 420 MPa. Grade 280, smooth No. 2 bars were used for the transverse reinforcement in the boundary elements of all walls. The welded wire reinforcement does not exhibit a well-defined yield point. Mean value of the measured mechanical properties of the deformed bars and wire reinforcement used in this study are shown in Table 3. Yield strength of wires was measured at 0.2% offset elongation. As can be seen in the table, the wire reinforcement shows limited ductility and low elongation at fracture.

Table 3 – Measured mechanical properties of the concrete mixtures

Mechanical property	No. 5	No. 3	No. 2	Cal. 8
Type	Deformed	Deformed	Deformed	Welded-wire reinforcement
Diameter (nominal), mm	15.9	9.5	6.4	4.1
Yield strength, f_y, MPa	411	435	273	630
Ultimate strength, f_u, MPa	656	659	388	687
Elongation at fracture, %	12.2	10.1	19.2	1.9

2.4 Ground motions and test protocol

Both, recorded and artificially generated ground motions were used in this study. The S90E component of the Caleta de Campos ground motion (CA-71) recorded during the January 11, 1997, Michoacan earthquake in Mexico (M_w = 7.1) was chosen as the base earthquake record. Using the CA-71 record as a Green function [10], two additional records, CA-77 and CA-83, were numerically generated to simulate larger magnitude earthquakes of M_w = 7.7 and M_w = 8.3, respectively. Table 4 shows the test protocol used for each of the wall specimens. A random acceleration signal (white noise, WN) at 0.01 g root mean square (RMS) was applied prior to and after each event in order to determine the periods of vibration and the damping factors of the specimens. All motions were applied at the wall base, in the in-plane direction of the walls.

2.5 Test setup and instrumentation

A mass-rig system for supporting the mass and transmitting the inertia forces was used for testing of walls. The device allows guided horizontal sliding of the mass within a fixed supporting structure installed outside the shaking table [9]. The fundamental period of vibration of a typical two-story height residential unit was estimated to be 0.12 sec [6]. Taking into account the scale factors of the simple law of similitude (1.25), isolated wall models were designed to achieve an initial in-plane period of vibration of approximately 0.12/1.25 = 0.10 sec. An axial compressive stress of 0.25 MPa was uniformly applied to the top of walls and kept constant during the tests. All specimens were densely instrumented internally and externally with various measuring devices.

Table 4 – Shake table test protocol

Event	Record	Target PGA		Total duration, s
		%	*g*	
0	WN	---	0.01	120.0
1	CA-71	50	0.19	29.5
2		100	0.38	
3	CA-77	75	0.54	36.1
4		100	0.72	
5	CA-83	75	0.98	99.8
6		100	1.30	
7		150	1.95	
8		200	2.60	
9		200-R1*	2.60	
10		200-R2*	2.60	
11	WN	---	0.01	120.0

*R1, R2 = First and second additional runs at 200% PGA of the CA-83 record.

3. Tests results and discussion

Wall response was assessed through cracking, failure modes, lateral drift components, changes in fundamental frequencies and damping factors as well as stiffness decay curves. The performance of walls is described in terms of three limit states: diagonal shear cracking, peak lateral resistance, and loss of lateral resistance. Diagonal shear cracking, DSC, was defined as the drift corresponding to the onset of inclined web cracking. Peak lateral resistance, PLR, was defined as the drift corresponding to the maximum lateral resistance of the walls. Loss of lateral resistance, LLR, was denoted as the drift corresponding to a decrease in peak lateral resistance of 20% in any direction of loading during the event.

3.1 Cracking and failure modes

All SFRC walls developed predominantly diagonal cracking, irrespective of the fiber type (1F or 2F) or volume content, with few flexural (horizontal) cracks. As was expected, the SFRC walls reached larger drift ratios as the fiber content increased, irrespective of the fiber type (Fig. 2a). However, fibers with a higher aspect ratio led to a greater number, smaller width cracks. The walls with deformed bars or welded wire reinforcement in the web showed a larger number and a more uniform distribution of cracks than the SFRC walls. In particular, the wall with deformed bars in the web developed the largest number of diagonal cracks than any of the other walls.

The failure mode of all SFRC walls may be described as diagonal tension. Failure was sudden and was triggered by the abrupt opening of one or two of the major diagonal cracks in the web. The wall reinforced with deformed bars exhibited a mixed failure mode, where diagonal tension and subsequent diagonal compression, were observed. Such a mixed failure mode was characterized by yielding of the web steel reinforcement followed by crushing of the concrete in the upper portion of the web. The failure mode of the wall with welded wire reinforcement was very sudden and occurred by diagonal tension along a major diagonal crack inclined at drifts smaller than any of the other walls.

3.2 Lateral drift components

Wall drift components from flexure, shear, and horizontal sliding at the base were calculated from the measurements obtained from the external transducers. A comparison between the measured total drift and that computed by the summation of each measured component showed discrepancies no greater than 9%. This discrepancy was distributed proportionally among the three deformation components. Fig. 2b shows the calculated contribution of each deformation component for the SFRC walls as a function of the factor [V_f (l_f/d_f)]. Linearly varying trend lines have been added to better visualize the overall tendency of each component.

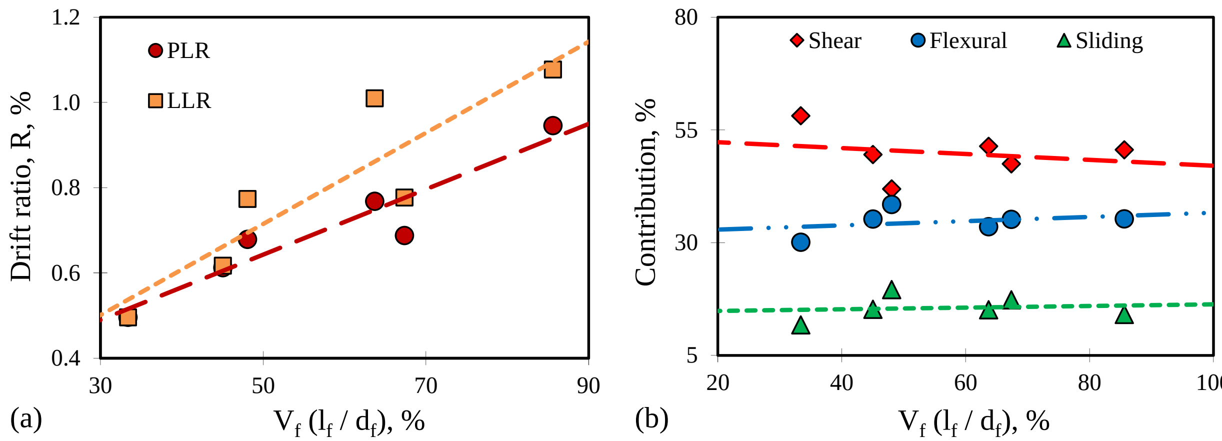

Fig. 2 – Influence of fiber volume and fiber type on drift ratio for SFRC walls: (a) drift ratio and [V_f (l_f/d_f)] relation at PLR and LLR, (b) percent contribution of flexural, shear, and horizontal sliding drift components as a function of [V_f (l_f/d_f)] at PLR.

As can be seen in Fig. 2b, shear distortion tended to decrease slightly as [V_f (l_f/d_f)] increased at peak lateral resistance (PLR). The contribution of horizontal sliding at the base was observed to be nearly the same for all SFRC walls. In other words, increasing fiber volume and fiber length to diameter ratio did result in better control and reduced shear distortions, as was expected, but the measured improvement was small for the fiber volumes and fiber types studied.

3.3 Vibration frequencies

The fundamental frequency of vibration and damping ratios of the walls were estimated from the ratio (transfer function) between the spectral amplitude (FFT) of the acceleration recorded at the top of the specimens and that recorded at the base (shake table). Ratios of spectral amplitudes for SFRC wall MC2F1.00 measured at the beginning of each event is shown in Fig. 3a. Also shown in the figure are the corresponding spectral amplitudes for the walls with deformed bars, MCN100 in Fig. 3b.

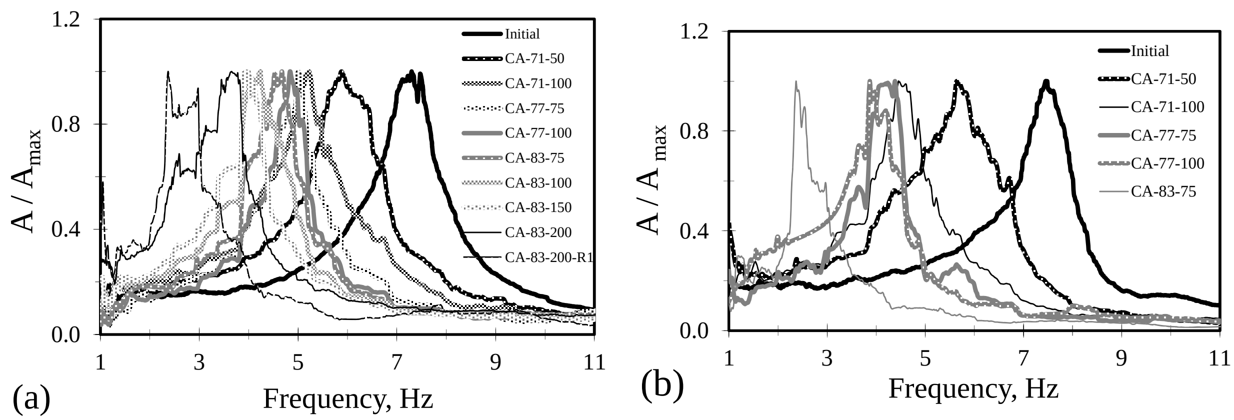

Fig. 3 – Ratios of spectral amplitudes of acceleration: (a) MC2F1.00, (b) MCN100.

For comparison purposes, spectral amplitudes in Fig. 3 were normalized by the peak spectral amplitude, A_{max}, of the event considered. To identify the frequency and damping factors, the procedure proposed by Rinawi and Clough [9] was used. In this approach, the transfer function of a single degree of freedom system is fitted to the experimental shape of a similar transfer function. The equivalent damping factor is then identified by means of the amplitude of the function related to the vibration mode under consideration. The effective damping factor was calculated by subtracting the value of damping generated in the LMGS of the mass-rig system, from the equivalent viscous damping involved in the measured response of the specimen. Carrillo and Alcocer [11] have demonstrated that the LMGS of the mass-carrying load system did not add any significant amount of damping into the specimen response (highest values of added damping lower than 0.20%).

The data in Fig. 3 show that the initial frequency (event 0, Table 4) was, on average, 18% lower than the target frequency of 10 Hz (0.10 s). This result is attributed mainly to the shrinkage cracking observed in all walls, prior to applying any motions. The data also show that the frequency of vibration of all walls was reduced significantly after the first event. Subsequent events resulted in further reduction of the vibration frequencies and thus the lateral stiffness of the walls as discussed next.

3.4 Stiffness decay

Based on the calculated frequencies, the reduction in stiffness of the walls after each event is shown in Fig. 4 as a function of lateral drift. These values were back calculated from the wall frequencies and thus they represent, in effect, the average secant stiffness of the walls measured during each event. It can be seen that after the first event (CA-71 at 50% amplitude), where maximum lateral drifts did not exceed 0.1%, degradation of the SFRC wall lateral stiffness was substantial, ranging between 30% and about 50% reduction with respect to the initial stiffness, K_o. Diagonal cracking of the walls during event 2 (shown by the shaded region labeled as DSC) further reduced wall stiffness to as low as 38% to 58% of their initial stiffness. These results show that stiffness reductions in the order of 50% can be expected at small lateral drifts (0.1 to 0.2%) for these SFRC walls. In practice, these drifts may be expected to be caused by relatively minor seismic events, which will significantly reduce the fundamental vibration frequencies (see Fig. 3).

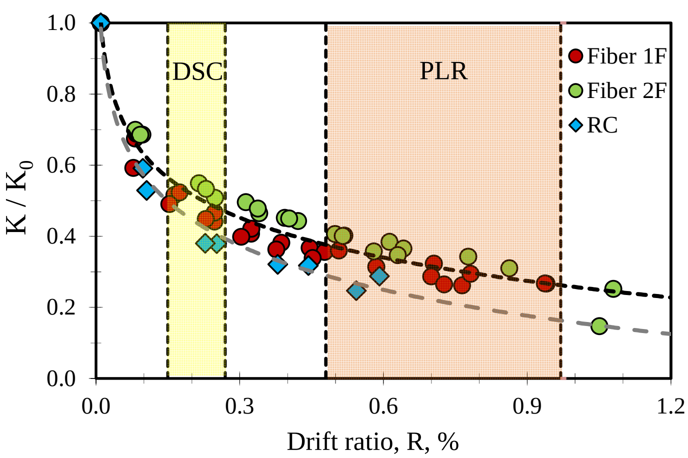

Fig. 4 – Stiffness degradation of walls based on measured frequencies.

After diagonal cracking, stiffness decay becomes less sensitive to increases in lateral drifts (see Fig 4). At peak lateral resistance (PLR), for example, the reduction in stiffness varied between 25% and 40% of the initial stiffness over a wider range of lateral drifts (between 0.42% and 0.97%). The observed reductions in stiffness at peak resistance are in line with those suggested for the analysis of walls with cracked sections for conventionally reinforced walls [12]. It is noted, however, that stiffness reductions reported here are computed with reference to the initial measured stiffness, not to the initial value based on gross properties as often recommended in guidelines. As noted earlier, the initial measured stiffness was about 10% smaller than that computed based on gross sections. Although the data undoubtedly show some scatter, the results show that the SFRC walls with fiber type 2F had smaller stiffness reductions than the SFRC walls with fiber type 1F and also smaller than those observed for the walls with either deformed bars or welded wire reinforcement over the entire range of lateral drifts.

3.5 Damping ratios

The calculated equivalent viscous damping ratios are shown for all SFRC walls in Fig. 5 a as a function of the maximum measured drift ratio in each event. As mentioned earlier, the procedure proposed by Rinawi and Clough [9] was used for identifying the damping factors. The corresponding values for the walls with deformed bars or welded wire reinforcement are shown in Fig. 5b. Trend lines corresponding to a potential regression of the data is also shown in the figure.

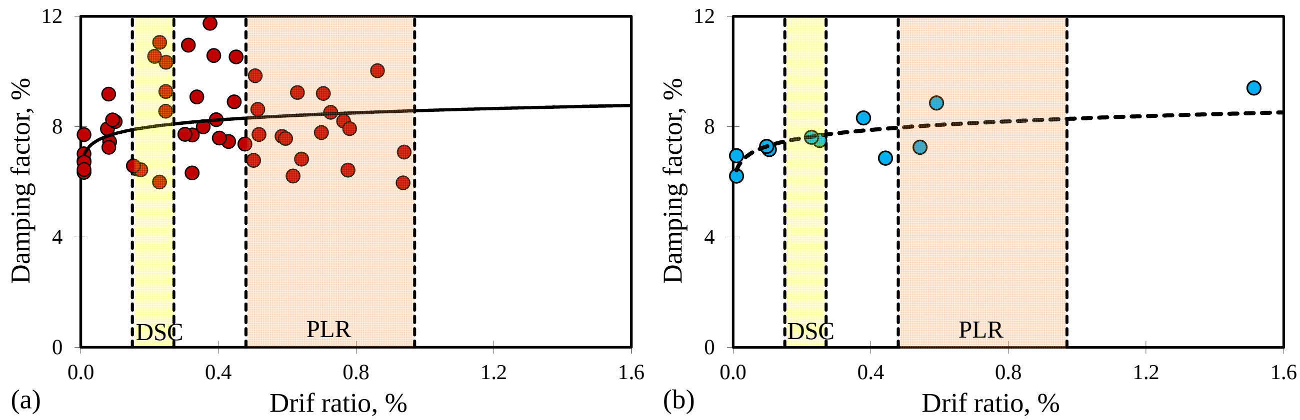

Fig. 5 – Calculated damping ratios (%): (a) SFRC walls and (b) walls with deformed bars or welded wire reinforcement.

The data show that the initial damping factor (measured during event 0, Table 4) varied between 6.3 and 7.7% for the SFRC walls (Fig. 5a), and between 6.2 and 6.9 for the walls with deformed bars or welded wire reinforcement (Fig. 5b). While the data show wide scatter (values corresponding to the six walls are included), the damping ratio tended to increase with increasing lateral drifts, as might be expected. For the SFRC walls, the largest damping values were calculated after diagonal cracking but prior to reaching peak lateral resistance, with damping ratios as high as 12%. Such values are lower than the damping ratios (close to 15%) measured during testing of conventionally reinforced walls [13]. After reaching peak resistance, damping ratios for the SFRC walls appear to decrease somewhat. This result suggests that a steel fiber mixture can be a substantial source of damping when the fibers are fully engaged (i.e., after cracking but prior to fiber pull out).

The calculated damping ratios for the walls with deformed bars or welded wire reinforcement also increased with lateral drifts, but they never exceeded 8% within the diagonal cracking and peak lateral resistance limit states. The maximum value was measured for the wall with deformed bars at very large drifts and only after substantial loss of lateral strength.

4. Final remarks

In this paper, the stiffness decay characteristics of six steel fiber reinforced concrete (SFRC) walls subjected to shaking table excitations is presented. Properties of two reinforced concrete (RC) walls tested under the same excitations are also included for comparison purposes. Lateral drift components, changes in fundamental frequencies, stiffness decay curves, and damping ratios are compared and discussed. Based on the observed behavior, the following findings and conclusions can be established.

The SFRC walls reached larger drift ratios as the fiber content increased, irrespective of the fiber type; however, fibers with a higher aspect ratio led to a greater number, smaller width cracks. Due to the shrinkage cracking observed in all walls, prior to applying any motions, the initial frequency of SFRC walls was, on average, 18% lower than the target frequency of 10 Hz. For the SFRC walls, the largest damping values were calculated after diagonal cracking but prior to reaching peak lateral resistance, with damping ratios as high as 12%. This result suggests that a steel fiber mixture can be a substantial source of damping when the fibers are fully engaged. For the conventionally RC walls, the calculated damping ratios also increased with lateral drifts, but they never exceeded 8% within the diagonal cracking and peak lateral resistance limit states.

SFRC walls showed that stiffness reductions in the order of 50% small lateral drifts (0.1 to 0.2%) such as those that might be expected during minor seismic events. Such stiffness reductions will change the vibration frequencies and must be considered, for example, in the assessment of the seismic response of existing construction that may have been subjected to past events. The data also show that the SFRC walls with fiber type 2F had smaller stiffness reductions than the SFRC walls with fiber type 1F and also smaller than those of the walls with either deformed bars or welded wire reinforcement over the entire range of lateral drifts.

5. Acknowledgements

The authors gratefully acknowledge the support of construction materials from Cemex Group (concrete) and Bekaert (steel fibers), as well as the extensive assistance in the experimental testing of staff and students of the Structural Engineering Laboratories of the Instituto de Ingeniería at UNAM. The first author expresses his gratitude to the Universidad Militar Nueva Granada (UMNG, Colombia) for sponsoring the research grant IMP-ING-2130.

6. References

[1] Carrillo J, Alcocer S, Pincheira J (2012): Shaking table tests of steel fiber reinforced concrete walls for housing. *15th World Conference on Earthquake Engineering*, 15WCEE, Lisbon, Paper 69.

[2] Susetyo J., Gauvreau P. and Vecchio F. (2011): Effectiveness of steel fibers as minimum shear reinforcement. *ACI Structural Journal*, 108:4, 488-496.

[3] Carrillo J (2015): Damage index based on stiffness degradation of low-rise RC walls. *Earthquake Engineering and Structural Dynamics*, 44, 831-848.

[4] Erberik M, Kurtman B (2010): A detailed evaluation on degrading behavior of structural systems. *9th U.S. National and 10th Canadian Conference on Earthquake Engineering*, Toronto, Canada, Paper 369.

[5] Petryna Y, Dfanner F, Stangenberg F, Kratzig T (2002): Reliability of reinforced concrete structures under fatigue. *Reliability Engineering and System Safety*; 77: 253-261.

[6] Carrillo J., Alcocer S (2012): Seismic performance of concrete walls for housing subjected to shaking table excitations. *Engineering structures*, 41, 98-107.

[7] American Concrete Institute, ACI (2014): Building Code Requirements for Structural Concrete and Commentary, ACI 318-14, Farmington Hills, MI.

[8] ASTM C-1609 (2012): Standard test method for flexural performance of fiber-reinforced concrete (using beam with third-point loading). West Conshohocken, PA, USA.

[9] Rinawi A, Clough R (1992): Improved amplitude fitting for frequency and damping estimation. *10th International Modal Analysis Conference*, Society for Experimental Mechanics, Bethel, CT, 893-898.

[10] Carrillo J, Rubiano A, Delgado E (2013): Evaluation of Green's functions when simulating earthquake records for dynamic tests. *Ingeniería e Investigación*, 33:3, 28-33.

[11] Carrillo J, Alcocer S (2011): Improved external device for a mass-carrying sliding system for shaking table testing. *Earthquake Engineering and Structural Dynamics*, 40:4, 393-411.

[12] Moehle J, Ghodsi T, Hooper J, Fields D, Gedhada R (2011): Seismic design of cast-in-place concrete special structural walls and coupling beams: A guide for practicing engineers, NEHRP Seismic Design Technical Brief No. 6, National Institute of Standards and Technology, Gaithersburg, MD, NIST GCR.

[13] Aristizabal-Ochoa J (1983): Cracking and shear effects on structural walls. *Structural Engineering, ASCE*, 109:5, 1267-1277.